SOLID STATE DYE SOLAR CELLS WITH METALLIC REGENERATORS: TOWARDS DEVICES WITH ENHANCED ACTIVE AREA

F.O. Lenzmann, C. Olson, P.Y. Pichon, B. Heurtault, M.J.A.A. Goris, T. Budel
ECN Solar Energy, Westerduinweg 3, NL-1755 LE Petten

ABSTRACT: In an alternative approach to solid state dye solar cells a molecular dye is situated at the interface between a TiO_2 film and a metallic (Au) film. In a proof of principle with flat model devices, we have shown earlier that the Au layer efficiently regenerates the charge-neutral state of the dye upon electron injection into the TiO_2 conduction band under illumination. For practically more relevant devices an increased active area is required for enhanced current output. A specially adapted TiO_2 morphology with nanotubular morphology can minimize reflection losses from the metallic regenerator. In this paper the preparation of such films on transparent SnO_2:F-coated glass substrates by electrochemical anodization of titanium layers is described. The focus is on preparative parameters with direct influence on film properties relevant to the application in solid-state dye solar cells (transparency and mechanical integrity of the layers).

Keywords: Dye-Sensitized, Fundamentals, TiO_2, Solid State

1 INTRODUCTION

Compared with liquid electrolyte based systems, solid-state dye sensitized solar cells (ss-DSC) offer the prospect of possible benefits in manufacturing processes, e.g., less stringent requirements for sealing and interconnection schemes on the module level. In the liquid electrolyte DSCs the presence of a corrosive liquid, containing iodine leads to the requirement of protective coatings for internal interconnects or current collector grids.

However, the solid state DSCs are currently at a significantly earlier research stage and still inferior to their liquid electrolyte counterparts both in terms of efficiency and stability.

The efficiency gap between the solid-state and liquid electrolyte based DSCs - best published data are 4 % vs. 11 % on small, sub-cm^2 surface areas - is explained primarily by the fact that the best performance of current ss-DSC devices is achieved with TiO_2 layers, which are only 2-3 µm thick [1]. This is about 5 times less than required for optimal light absorption with typical dye sensitizers (maximum absorption coefficients are in the range of $1\text{-}2\cdot10^4$ $M^{-1}cm^{-1}$). This undesirable thickness limitation of the TiO_2 layers is related to an unoptimized kinetic competition between charge transport and interfacial recombination [2] as well preparative challenges to achieve complete pore-filling of the regenerator into the porous TiO_2 films [3].

Our approach for applying a (noble) metal regenerator in ss-DSCs can be expected to influence the kinetic balance between charge transport and interfacial recombination and aims at robust long-term stability. We have shown earlier that the application of a metallic Au film leads to efficient regeneration of the charge-neutral state of the dye [4] in flat model systems. For current generation superior to the output of a dye monolayer on a flat TiO_2 surface a morphology with substantially enhanced active area is required.

The application of a reflective regenerator in TiO_2 films with enhanced active area implies challenges for the device optics. In the case of disordered colloidal TiO_2 films, typically applied in DSCs, a metallic regenerator - interpenetrating the nanoparticulate TiO_2 network - would lead to substantial reflection losses at the side of light incidence (see figure 1). For the minimization of reflection losses it is therefore essential to apply TiO_2 films with an ordered, linear pore morphology on a transparent substrate - nanotubular TiO_2 films offer appropriate geometrical properties.

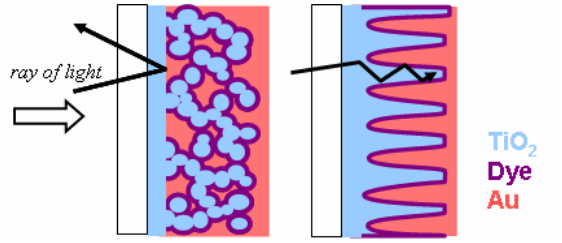

Figure 1: Optical losses from a reflective regenerator in a disordered colloidal TiO_2 film (left) can be minimized in TiO_2 films with an ordered, linear morphology (right).

The preparation of TiO_2 nanotubular films on transparent conductive oxide (TCO) substrates has been published only recently [5]. Such layers have been successfully applied to liquid electrolyte DSC [6,7], where they have shown beneficial slower interfacial recombination kinetics compared with nanoparticulate, colloidal TiO_2 films [7]. Such beneficial electronic properties are of particular interest for ss-DSC concepts, where in addition, the ordered, linear pore morphology may be beneficial for pore-filling.

Here we describe the preparation of such films using electron beam evaporated titanium layers. We discuss the importance of defining an appropriate end point of the anodization process in order to obtain transparent layers while maintaining their mechanical integrity.

2 EXPERIMENTAL

2.1 Preparation of titanium layers on SnO_2:F-coated glass substrates suitable for electrochemical anodization

All samples of this study are prepared on Pilkington SnO_2:F glass (nominal sheet resistance 15 Ω/sq). The dimensions of the substrates were 1 cm x 10 cm. After careful cleaning of the substrates using isopropanol and

de-ionized water the samples are left to dry in air. A compact TiO_2 buffer layer of 50 - 100 nm thickness is prepared by spray pyrolysis at a temperature of 450 °C, in which a precursor solution containing 200 mM titaniumtetra-isopropoxide and 400 mM acetylacetone in ethanol is sprayed onto the SnO_2:F-coated glass substrates, placed on a hotplate. The spraying procedure is essentially that described in reference [8].
After cooling down of the substrates, a titanium layer is deposited by electron-beam evaporation. Typically 2 µm thick layers were grown showing good substrate adhesion. After electron beam deposition the samples were cut to dimensions of 1 cm x 2 cm for the anodization experiments
Layers, which were not used immediately after the titanium deposition were stored in an argon glove-box in order to avoid oxidation of the titanium surface.

2.2 Preparation of TiO_2 nanotubes by anodization of titanium layers on SnO_2:F-coated glass substrates
The anodization of the films follows essentially the recipe by Schmuki [9]. The electrolyte solvent was ethylene glycol containing 0.3 wt% ammonium fluoride and 2 wt% water. All chemicals were from Sigma-Aldrich and used as received. The reactions were carried out in 50 ml beakers (with typically 35 ml electrolyte) using a 2 electrode set-up at room temperature and without stirring.
A Pt foil was used as counter electrode.
The samples and the Pt foil were contacted by crocodile clips and placed in the electrolyte in a vertical position with at distance of ~ 0.5 cm to each other with the crocodile clips about 3 mm above the electrolyte meniscus. The power supply was a E3647A model from Agilent. Anodizations were carried out via a PC using Labview, also allowing to record the anodization current as a function of time. A voltage ramp of 1V/s was applied in the beginning of the process until reaching the desired final voltage (35 V), which was then kept constant until the end. After anodization, the samples were rinsed in deionized water - followed in some cases by sonication in water using a 30W sonication bath for up to 15 min. The samples were finally dried in a stream of nitrogen and sintered at 450 ºC in air for 3 hrs.

2.3 Scanning electron microscopy
The morphological properties of the layers were characterized by scanning electron microscopy using a JEOL JSM6330 apparatus.

3 RESULTS AND DISCUSSION

3.1 Relation between current-time curves of the anodization current and some film properties

By comparing the two current-time curves in figure 2, it appears that the mechanism of nanotube formation on SnO_2:F/TiO_2 coated glass substrates follows that on Ti foils with the exception of a distinct current rise at the end of the anodization (for in-depth mechanistic interpretations of the current-time curves the reader is referred to ref [9]. The endpoint is a much more critical parameter for thin titanium films on SnO_2:F/TiO_2 coated glass substrates than for foils, which offer a virtually infinite supply of titanium.

If the anodization on the SnO_2:F/TiO_2 coated glass substrate is allowed to continue after there is Ti metal available as a reactant, the etching will consume any available TiO_2 until the SnO_2:F layer is exposed to the electrolyte. This is observed by a relatively sudden increase in the current as the insulating layer on the SnO_2:F is consumed, and by bubble formation on the surface from excess oxygen, as the oxidation of titanium ceases but water splitting continues to occur. This particular behavior is observed here after about 6000 s anodization time (see figure 2).

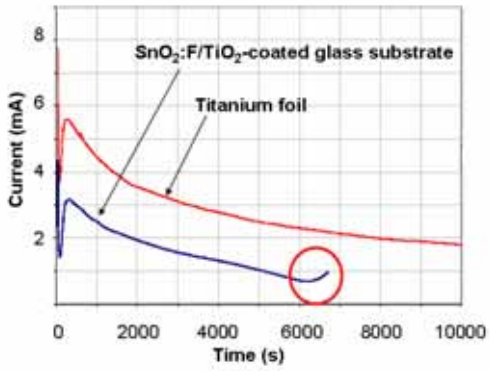

Figure 2: Characteristic current rise at the end of the anodization carried out on SnO_2:F/TiO_2-coated glass substrates

The described processes lead to the occurrence of a fully transparent zone, developing first at the bottom edge of the samples in the unstirred solution and progressing toward the top of the sample. This is consistent with thermal convection resulting from the exothermic oxidation reaction. (when stirred, the transparency initiated at the upstream edge and moved across the sample.)
Full mechanical integrity and transparency of the films after the anodization and annealing steps can be reached when the anodization process is ended at the beginning of the current rise with last traces of titanium metal still remaining in the film. When the anodization is ended before that point, some parts of the remaining titanium are not oxidized during the annealing, such that full transparency is not reached. When continuing the anodization beyond that point, delamination of the nanotube layers in the anodization bath or during the annealing occurs. The sketch in figure 3 illustrates these different growth states at the end of the anodization process with different amounts of remaining titanium in the layer.
The ideal endpoint is defined when the last monolayer of Ti atoms are oxidized, and the substrate is transparent and uniformly covered by TiO_2 nanotubes. The control of this endpoint depends on the homogeneity of the electrochemical cell, which is currently further optimized.

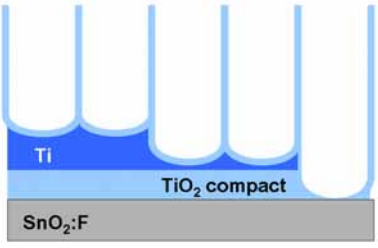

Figure 3: Different growth states of the nanotubes at the end of the anodization process.

3.2 Surface morphology

An open pore structure is observed at the top of the nanotubular TiO_2 films after anodization and annealing as shown in figure 4. Some smaller surface artefacts can be observed in figure 4A (ridges between the openings of the pores). As also described in previous work by other groups [9] such artefacts can be removed by mild sonication (4B).

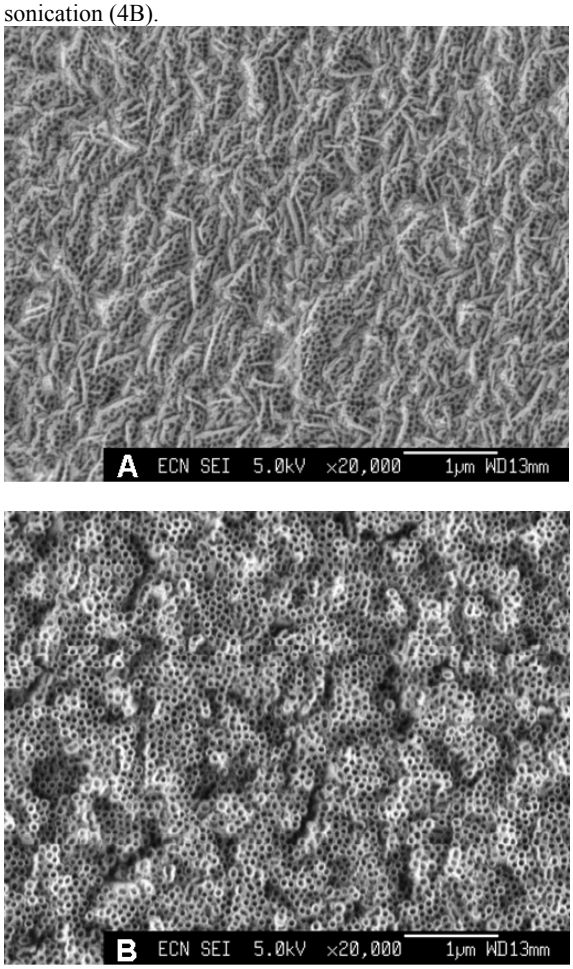

Figure 4: SEM micrographs of nanotubular TiO_2 layers (top views) before(A) and after (B) mild sonication.

3.3 Initial application of TiO_2 nanotubes to liquid electrolyte DSCs

Preliminary tests for the application of the nanotubular layers in DSCs were undertaken. Standard components for liquid electrolyte cells were used (dye N719, electrolyte containing 0.5 M HMII, 0.1 M LiI, 0.05 M I2, 0.5 M tbp in acetonitrile). The thickness of the nanotubular layer was ~ 3 μm, resulting in an optical density of ~ 0.3 at the absorption maximum of the N719 dye (535 nm). Reasonable photovoltaic characteristics with a good V_{OC} value were obtained (figure 5)

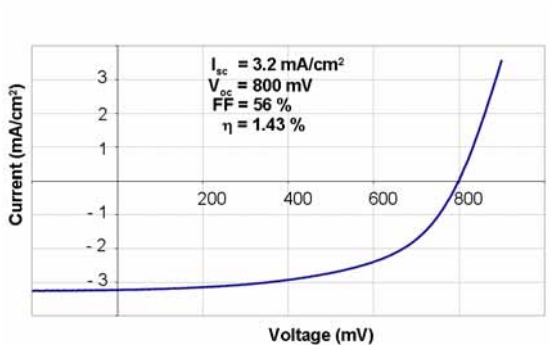

Figure 5: IV characteristics of a liquid electrolyte DSC with a nanotubular TiO_2 film

5 CONCLUSIONS

We have shown the preparation of nanotubular TiO_2 films by electrochemical anodization of electron beam deposited titanium films on transparent SnO_2:F/TiO_2 coated glass substrates. Mechanically robust and transparent nanotubular films can be prepared, when an appropriate end-point of the anodization process is chosen. The control of this end-point is currently further optimized.

The geometrical and optical properties of these layers (opened and linear pores, high surface area and transparency) are well suited for application in solid-state dye solar cells in general and for application of reflective regenerators, like Au, in particular. Preliminary tests of the nanotubular films in liquid electrolyte DSCs were successful.

5 REFERENCES

[1] M. Graetzel, MRS Bulletin 30 (2005) 23
[2] B. O'Regan, F. Lenzmann, J. Phys. Chem. B 108/14 (2004) 4342
[3] L. Schmidt-Mende, M. Graetzel, Thin Solid Films 500/1-2 (2006) 296
[4] F.O. Lenzmann, B.C. O'Regan, J.J.T. Smits, H.P.C.E. Kuipers, P.M. Sommeling, L.H. Slooff, J.A.M. van Roosmalen, Progress in Photovoltaics: Research and Applications 13 (2005) 333
[5] G. Mor, O. Varghese, M. Paulose, C. Grimes, Adv. Funct. Mater. 15 (2005) 1291
[6] G. Mor, K. Shankar, M. Paulose, O. Varghese, C. Grimes, Nano Letters 6/2 (2006) 215
[7] K. Zhu, N. Neale, A. Miedaner, A. Frank, Nano Letters 7/1 (2007) 69
[8] L. Kavan, M. Graetzel, Electrochimica Acta 40/5 (1995) 643
[9] J. Macák, P. Schmuki, Electrochimica Acta 52 (2006) 1258